



# Postural control in paw distance after labyrinthectomy-induced vestibular imbalance

Gyutae Kim<sup>1</sup> · Nguyen Nguyen<sup>1,2</sup> · Kyu-Sung Kim<sup>1,2</sup>

Received: 28 January 2020 / Accepted: 14 October 2020  
© International Federation for Medical and Biological Engineering 2020

## Abstract

Balance control is accomplished by the anatomical link which provides the neural information for the coordination of skeletal muscles. However, there are few experimental proofs to directly show the neuroanatomical connection. Here, we examined the behavioral alterations by constructing an animal model with chemically induced unilateral labyrinthectomy (UL). In the experiment using rats (26 for UL, 14 for volume cavity, 355–498 g, male), the models were initially evaluated by the rota-rod (RR) test (21/26, 80.8%) and ocular displacement (23/26, 88.5%). The duration on the rolling rod decreased from  $234.71 \pm 64.25$  s (4th trial before UL) to  $11.81 \pm 17.94$  s (1st trial after UL). Also, the ocular skewed deviation (OSD) was observed in the model with left ( $5.79 \pm 3.06^\circ$ ) and right lesion ( $3.74 \pm 2.69^\circ$ ). Paw distance (PW) was separated as the front (FPW) and the hind side (HPW), and the relative changes of HPW ( $1.71 \pm 1.20$  cm) was larger than those of FPW ( $1.39 \pm 1.06$  cm), providing a statistical significance ( $p = 1.51 \times 10^{-4}$ , *t* test). Moreover, the results of the RR tests matched to those of the changing rates (18/21, 85.7%), and the changes (16/18, 88.9%) were dominantly observed in HPW (in FPW, 2/18, 11.1%). Current results indicated that the UL directly affected the changes in HPW more than those in FPW. In conclusion, the missing neural information from the peripheral vestibular system caused the abnormal posture in HPW, and the postural instability might reduce the performance during the voluntary movement shown in the RR test, identifying the relation between the walking imbalance and the unstable posture in PW.

**Keywords** Balance · Paw distance · Posture · Voluntary movement · Unilateral labyrinthectomy

## 1 Introduction

Accumulated neuroanatomic results indicate that the skeletal muscles receive the motor commands from the central nervous system to support the balance of posture or voluntary movement. The neural control using the commands is a complicated process, mainly constructed by the combination of visual, somatosensory, and vestibular information [1–3]. Based on the evoked body sway, center of mass or center of pressure in human and other species, these control systems

have been thoroughly investigated separately in visual [4, 5], somatosensory [6, 7], and vestibular sensations [8, 9]. These previous studies indicated that the balance-related motor command modified its amplitude to provide the neural information for a fast balance [5]. Also, the sensations with different neural orientations were interacted to coordinate the muscular activities [10], and their relevant motor commands possessed various sensations from different portions. According to the studies of vestibular compensation, some patients showed their recovery in the postural balance by utilizing the remaining sensations, which was covered by one or multiple missing information. Especially, the combination of various sensations was easily observed in vestibular hypermetria, which might be resulted from the reduced neural inhibition in the cerebellum to generate the motor command in the spinal motor system [11]. Many previous studies supported this addressed process by showing the relation between the abnormal vestibular function and the head movement [12–14].

In the model with unilateral vestibular loss, the initial change was observed in the neural activities in vestibular

✉ Gyutae Kim  
kimg@inha.ac.kr

<sup>1</sup> Research Institute for Aerospace and Medicine, Inha University, JungSeok Bldg. B-501, 366 SeoHae-daero, Joong-gu, Incheon 22332, South Korea

<sup>2</sup> Department of Otolaryngology Head & Neck Surgery, Inha University Hospital, 27 Inhang-ro, Jung-Gu, Incheon 400-711, South Korea

nuclei (VN) by decreasing or increasing the neural activity in the sides with lesion or non-lesion, respectively [14]. The asymmetric neural information by the unilateral vestibular loss affected the modulation of a motor command to provide the balance control, and it directly caused an abnormal kinetic response. For the assessment of the dysfunctional kinetic activities, various behavioral tests as well as rota-rod (RR) test have been widely used in animal experiments [15–17]. However, few dynamic results have revealed this neuroanatomically relayed cause and effect, which directly indicates from the vestibular loss to an abnormal activity during posture and voluntary movement. Moreover, insufficient experimental evidence to support the neuroanatomical and behavioral links was often underestimated in model evaluation, and it eventually produces the uncertainty in the coordination in motor control by the neural information. In a quadruped animal, for instance, the postural balance and the stable movement was successfully constructed by the fine control of four paws, and the neural information initiated in VN generated the requisite motor command for the kinetic consequence. In addition, the control of paws was possibly identified by their continuous relocation, which could be assessed by their paw distance (PW) [18]. Thus, an incomplete motor command by a damaged sensory signal results in abnormal balance and unstable motion, and the dysfunction by a loss of sensory information can be assessed by measuring the relocation of paws. Some previous studies attempted to show the muscular control to maintain a stance with no correlation with the neuroanatomical link [18–20]. According to these studies, the muscular responses to a perturbing plane showed the mechanical strategy for the postural and the motional balance with no deliberation on its initiation, the neural motor command.

To overcome the weak proof ranged from the neural origination to the abnormal behavioral responses, we constructed an animal model with unilateral vestibular loss. For the consistent and easy model generation, chemical unilateral labyrinthectomy (UL) was performed for the vestibular loss. An animal model was evaluated by RR and ocular skewed deviation (OSD) tests, and their results verified a reliable model construction. PW between two paws in front or hind side identified the modification in the animals' behaviors, and it provided a directly affected body area by the unilateral vestibular loss. According to the current results, the unilateral vestibular loss serially affected the initial motor command, the transferred neural information, and the muscular activities, implying the direct vestibular effects for the balance of posture and voluntary movement. In addition, the results suggested a possible reason to explain the reduced walking performance after UL, which was related with PW.

## 2 Methods

Overall experimental process was separated into three steps; behavioral test before UL, animal model construction, and behavioral test after UL. In each behavioral test, we conducted three independent tests: PW, RR, and OSD. By comparing the difference in the given behaviors before and after UL, we assessed the effects by unilateral vestibular dysfunction and its relevant kinetic consequences.

### 2.1 Animal preparation

UL was performed by an intratympanic injection of ferric chloride ( $\text{FeCl}_3$ ) into the middle ear (ME) cavity of rodents (SD rat, male), and  $\text{FeCl}_3$  was injected as the form of a toxified solution mixed with saline (0.69 g/ml,  $\text{FeCl}_3$  /saline). An animal was anesthetized by an intramuscular injection of a mixture of ketamine (1  $\mu\text{l/g}$ ) and xylazine (0.33  $\mu\text{l/g}$ ). To find a proper amount of the toxified solution, the volume of ME cavity was measured by initially injecting saline under a microscope. The intratympanic injection was made by a syringe (0.5-mm diameter needle) advancing through the tympanic membrane until its tip encountered the middle-ear ossicles. Once positioned, the needle was slightly pulled back, and the injection started. Saline was injected until it was flowed back through the tympanic membrane. When the injecting saline leaks back through the tympanic membrane, the injection was stopped, and the injected volume of the solution was measured. Based on the measured volumes in different animals, an averaged volume was determined, and the same amount of  $\text{FeCl}_3$  solution was applied to construct a UL model. After the injection, the animal was left to recover from anesthesia. All experimental procedures and the laboratory animal care in this study were verified and approved by University Animal Ethics Committee.

### 2.2 Paw distance

PW indicates the distance between two legs from the front or the hind side of an animal, separately, and each animal underwent two independent recording sessions before and after UL. Thus, there were two different kinds of PW: the front (FPW) and the hind paw distances (HPW). To measure them, a simple device was designed, composed of a transparent box ( $L \times W \times H = 25 \times 19 \times 21$  cm), a camera, and a rectangular parallelepiped-shaped structure ( $L \times W \times H = 28 \times 27 \times 65$  cm). The box was mounted on top of the structure, and the camera was located between the box and the bottom of the structure. The camera continuously recorded all the positions of the animal's paws ( $> 180$  s, 28 frames/s) during the sessions. The video format captured by the camera was *RGB24*, and its size was  $1280 \times 720$  (width  $\times$  height). Before the animal awaked from anesthesia, two different colored scraps

were attached on the bottoms of paws; the green color on the front and the orange on the hind paws. Then, the animal was placed in the transparent box for the recordings. Once completing the recording session, the movie files were processed to compute PW in a customized code (see “Data analysis”). After the recording was completed, the animal started additional tests, such as RR and OSD tests for a model conformation.

### 2.3 Rota-rod test and ocular displacement

Additional observations were made for the confirmation of a model; one was RR test and the other was the identification of the ocular displacements. RR test was conducted to measure how long an animal maintained to walk on a rolling rod. After the PW measurement was done, RR test was performed with a constant speed (34 m/min). The test lasted during an approximate 3-min period while the animal could maintain RR test, and this process repeated up to four times with a 5-minute break. During the process, the test was terminated if the animal changed its walking direction oppositely or the animal was just hanging the rolling rod with no walk. The attained time (second) on the rod was measured, and the results indicated as the performance of the walking balance.

Ocular displacement was observed immediately after an animal model was awakened from the anesthesia. Generally, the ocular positions were skewed after UL; the eye of the lesion side by the toxic injection moved to the downward while the other side shifted to the upward direction, so-called OSD. This phenomenon indicates that the eyeball at each side rotated to a specific direction closely related with the lesion side. In this study, the lesion implied the physical damage on the hair cells in labyrinth by injecting  $\text{FeCl}_3$ . As the ocular skewness disappeared between 24 and 72 h after awakened from the anesthesia, the animal’s facial pictures were taken for the measurement of the ocular tilted degree before and after UL.

### 2.4 Data analysis

PW was obtained based on the image processing of color detection. For the data preparation, the recorded movie file was separated into multiple pictures, and specific colors (the green and the orange colors for the front and the hind paws, respectively) were detected in each picture. Once a picture was loaded, a pre-defined marker was applied for the detection; 8-pixel area for marker size across a color range of 15 intensity values from the original RGB value. The initial color of target was identified using a free software (color cop), and we used the color range to accept some errors from the initial color. The first identified position was used as a reference to calculate the possible PWs (mm), and all distances in each picture were saved for a total population of PW. To avoid

the possibility to include the distances by two positions on a paw, the distances shorter than the longest distance in one sole of a foot were discarded. In all separated pictures, the same processes were conducted, and the accumulated PWs were presented in a histogram to visualize the calculated PWs. To assess the effects on PW by UL, the maximum PWs before and after UL were measured and their differences (PWD) were calculated. Using the obtained values, the changing rate in PW was computed as the following eqs. 1 and 2.

$$PWCR_{\text{front}} = 100 \times \left( 1 - \frac{FPW_{\text{before}} - PWD_{\text{front}}}{FPW_{\text{before}}} \right) \quad (1)$$

$$PWCR_{\text{hind}} = 100 \times \left( 1 - \frac{HPW_{\text{before}} - PWD_{\text{hind}}}{HPW_{\text{before}}} \right) \quad (2)$$

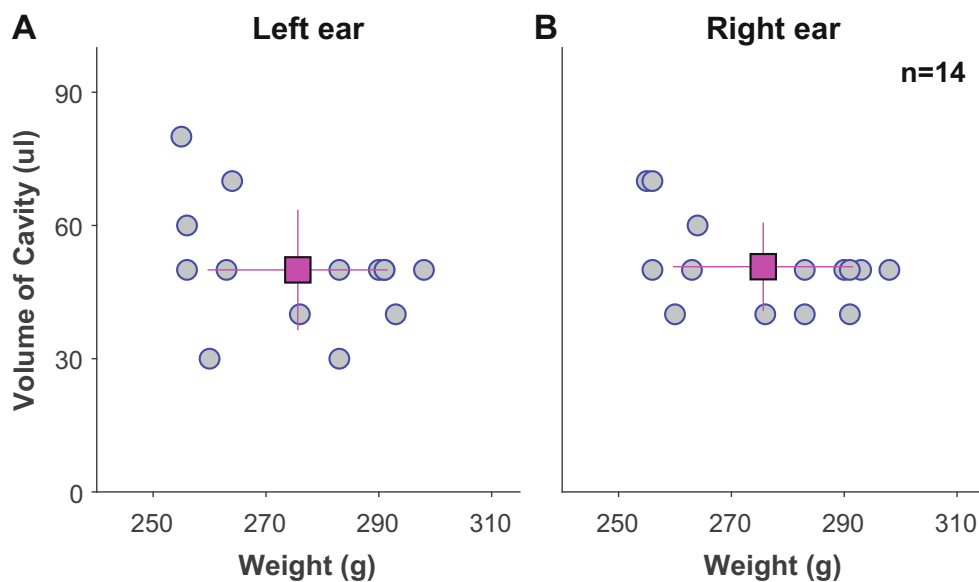
where  $PWCR_{\text{front}}$  and  $PWCR_{\text{hind}}$  are the changing rates in front and hind limbs, and  $PWD_{\text{front}}$  and  $PWD_{\text{hind}}$  are the PW differences in front and hind limbs, respectively.  $FPW_{\text{before}}$  and  $HPW_{\text{before}}$  are the front and the hind paw distances before UL, respectively.

OSD was measured using the pictures before and after UL. In each picture, a horizontal line connecting two eyes was drawn, and the inner angle between two obtained lines was measured to specify the degree of the ocular tilt. In case that the horizontal line of the normal condition was not perfectly horizontal, the degree of tilt was modified by rotating the horizontal line, and the same amount of adjustment was applied on that of the lesion-conditioned animal before the measurement of their inner angle. Depending on the direction of rotation from the horizontal line of the normal condition, its sign was determined; a positive for clockwise and a negative for count clockwise rotation. For example, the right eye moved to downward direction while the left eye rotated to upward direction under the right lesion. Thus, the sign of skewness for the animal with the right lesion was positive based on the subject’s viewpoint.

## 3 Results

Forty animals (355–498 g) were used for this study. Using 14 animals, the volume of cavity was measured by injecting the saline (see “Animal preparation”). The volume of cavity was separately measured in left and right ears, and their averages and standard deviation were calculated. The volumes of cavities in the left and right ears were similar ( $50 \pm 13.59 \mu\text{l}$  and  $50.71 \pm 9.97 \mu\text{l}$ , respectively). Therefore, the amount of a solution to fill the cavity was determined as the averaged value of the left and the right ears,  $50.35 \mu\text{l}$ , and our practical value was approximately  $50 \mu\text{l}$ . Due to the different size of animals, the volume of cavity was examined based on the animal weight, and its result showed that there was no relation between the cavity and the weight (Fig. 1). Based on the current

**Fig. 1** Volume of cavity. **(A)** The volume of the left ear cavity was presented based on the animals' weights. Each blue-edged circle indicated an individual measured volume depending on its weight. Their averages and standard deviations were calculated, and they were shown in a square (magenta) and a line, respectively. **(B)** The volume of the right ear cavity was displayed with the relation to the weights. The format of figure was the same as the other side, and the volume was a little larger than the other. The total number of animals was 14 ( $275.64 \pm 15.99$  kg, males), and the left and the right volumes were  $50 \mu\text{l}$  ( $\pm 13.59$ ) and  $50.71 \mu\text{l}$  ( $\pm 9.97$ ), respectively



relation between the cavity and the weight, the injecting volume of the toxic solution was maintained as the calculated value,  $50.35 \mu\text{l}$  ( $50 \mu\text{l}$ , practically).

Two types of behavioral tests (RR and OSD) were adopted to evaluate the constructed model. Out of 26 animals, 21 animals (80.8%) were used to test their walking balances on the rolling rod. The maintaining time on the rod increased as the trials were repeated. The initial averaged time was  $139.90 \pm 79.98$  s, and it reached to  $234.71 \pm 64.25$  s in four trials. Even though the maintaining time on the rod might be affected by the behavioral characteristics of each animal, it was consistently true that the tendency of the increasing time by the repetition of the test was applicable in all animals before UL. After UL, on the other hand, the duration on the rod dramatically dropped. The initial time on the rod after UL was  $11.81 \pm 17.94$  s, and it rarely changed during the repetition ( $8.62 \pm 8.67$ ,  $8.95 \pm 11.68$ , and  $7.48 \pm 7.83$  s for 2nd, 3rd, and 4th trials, respectively) (Fig. 2a). During the repetition of tests, there was no recovery in the result of RR test, indicating that the animals' walking balance was affected by UL. The similar consequence by UL was also identified in OSD. In the measurement of the ocular displacement after UL ( $n = 23$ , 88.5%), the initial ocular positions were tilted into downward or upward depending on the lesion side. After right UL, for instance, the position of the right eye moved to the downward while that of the left eye moved to the upward when UL was conducted on the right side. Therefore, the ocular displacement resulted in a positive tilt by a clockwise rotation after right UL. In the left UL, on the other hand, the eye movement was opposite after UL, and it caused a counterclockwise rotation, producing a negative tilt after left UL (see "Data analysis"). Using the same method, OSDs in 23 animals were measured (Fig. 2b). The OSD after left UL was ranged from  $2.77$  and  $13.57^\circ$  (mean  $\pm$  STD =  $5.79 \pm 3.06^\circ$ ), and that after right

UL was between  $2.78$  and  $8.20^\circ$  ( $3.74 \pm 2.69^\circ$ ). Compared with the averages, OSD from left UL was bigger than that from right UL. Also, this difference was maintained after removing one outlier (OSD =  $13.57^\circ$ ) of left UL, resulting in  $5.08 \pm 1.91^\circ$ .

PW was separately presented in front (Fig. 3a, left) and hind paws (Fig. 3b, left). Their maximums before (blue) and after UL (red) were used to show the effects by UL, and the differences before and after UL were indicated by the green circles. In addition, the changing rates were calculated (Eqs. 1 and 2), and they were presented in yellow-edged bars (Fig. 3a and b, right). Based on the PWs before UL, FPW ( $14.97 \pm 1.58$  cm) was wider than HPW ( $5.18 \pm 1.36$  cm), and this inequality between FPW and HPW was maintained after UL ( $14.99 \pm 2.09$  cm and  $6.75 \pm 1.27$  cm for FPW and HPW, respectively). Comparing the difference between FPW and HPW, the difference in HPW ( $1.71 \pm 1.20$  cm) was bigger than that in FPW ( $1.39 \pm 1.06$  cm), but the physical difference was not big enough to appreciate the effect by UL. Statistical examination ( $t$  test) compared 3 aspects of PW before and after UL: the range between the minimum and the maximum of PW, the minimum of PW, and the maximum PW. The statistical tests indicated that HPW was mainly affected by UL ( $p < 0.0001$ ) while FPW rarely showed the UL effects ( $p > 0.363$ ), agreeing with our current finding. Especially, the result was clearly recognized in the minimum or the maximum of PW, instead of their ranges. To emphasize the difference in FPW and HPW after UL, we examined the portion of the difference in PW (see "Data analysis"). The changing rates in percentage demonstrated the change in HPW was larger than that in FPW by UL ( $p = 1.51 \times 10^{-4}$ ,  $t$  test). This result indicated that UL affected the changes in HPW more than those in FPW, agreeing with their raw data. Using the changing rates in PWs, some insignificant results by RR tests

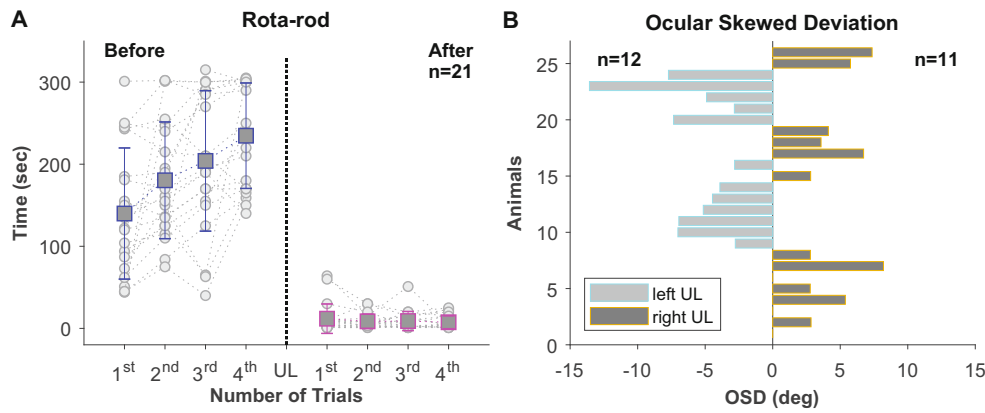


**Fig. 2** Behavioral responses in rota-rod (RR) tests and ocular skewed deviation (OSD). **(A)** The times on the rolling rod were presented before and after UL. For each, four independent tests were conducted (gray circles), and their averages and standard deviations were shown in a blue-edged and magenta-edged square and a line before and after UL, respectively ( $n = 21$ ). **(B)** OSD indicated the rotational angles caused by

the vertical ocular movements after UL. Due to the opposite moving directions of the lesion and the non-lesion sides, the counter-clockwise (negative) and the clockwise ocular tilts (positive) occurred in left (cyan-edged bar,  $n = 12$ ) and right UL groups (orange-edged bar,  $n = 11$ ), respectively. Total 23 animals were used for the measurements of OSD

were re-examined if the results were consistent. Three (3/21, 14.3%) cases were resulted in no significance ( $p > 0.058$ ,  $t$  test) in the RR test. Their corresponding changing rates were 4.88, 3.82, and 16.47% for FPW and 0.20, 62.31, and 19.02% for HPW, suggesting that our current analysis using PW strengthened the reliability in the behavioral tests after UL confirmation. In most significant data (18/21, 85.7%), the

significance in RR tests matched to the results in the changing rates. The dominant changes (16/18, 88.9%) occurred in HPW while only several cases (2/18, 11.1%) showed that the changing rates in FPW were bigger than those in HPW. This result also supported that the damages on the peripheral vestibular system mostly affected the abnormal motor control in hind rather than front side.

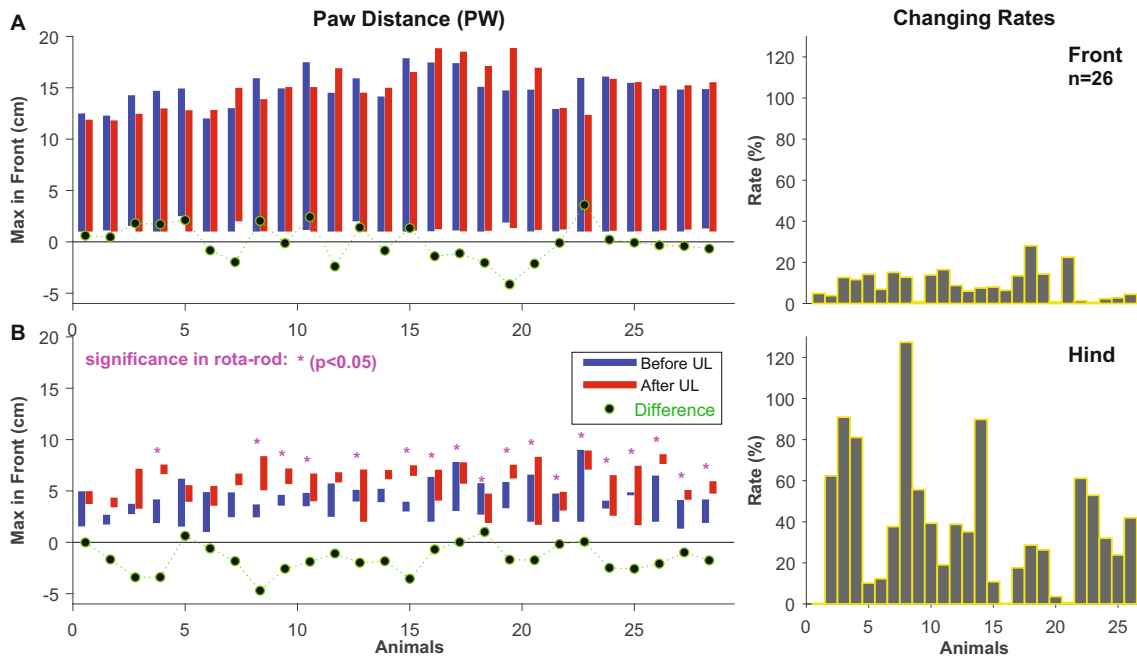


**Fig. 3** Paw distance (PW) and its changing rates in the front (A) and hind paws (B) ( $n = 26$ ). **(A)** The PWs from the front side were displayed. On the left in each figure, the PWs in each side were measured to obtain its values of minimum and maximum, and the information of PWs was used to present the change after UL. The difference (green-edged circle) between two maximums before and after UL was calculated and overlapped

on the same figure. On the right of the figure, the changing rates (yellow-edged bar) were presented, which were computed by the eq. 1. **(B)** The PWs from the hind side were shown in the same format as (A). In addition to the PWs and their differences, the statistical information was marked by \* (magenta) as the significant signs

## 4 Discussion

The physical damages to the vestibular end organ weakened the functional behaviors, losing the balance control in the posture and the voluntary movement. The generated damage was indicated in the decreasing RR time after UL, and the results implied the lack of a learning process as generally observed in the repeated trials on the rota-rod. This inference was reasonable as considering the unbalanced neural information in the central vestibular system by UL, which eventually resulted in abnormal PW. Our current results showed that the unstable walking balance was clear after UL, and its main cause was initiated by the abnormal PWs. Due to the vestibular damage, the partial loss of the relevant neural commands resulted in the walking control, which required the rhythmical coordination by the paws and their connected ankles. Accumulated neuroanatomical evidence has suggested the serial neural signals from the vestibular end organ to their skeletal muscles in the hindlimb possibly explained the imbalance of PW after UL [21–24], and the most relevant muscles were known as soleus and medial gastrocnemius (GL) [25–27]. Although there are still arguments related with the nature of neural signals, the serial process for the postural stabilization is generally agreed by the postural sensation to the muscular activities in the limbs [27].

The neural link from a motor command to its correlated muscular activity was the fundamental mechanism in the behavioral consequence, but few studies to deal with the whole link resulted in its insufficient comprehension. According to the accumulated neuroanatomical proofs, the integrated neural information from various peripheral sensory signals finely controlled the muscular responses, and the supervised muscular activities achieved the postural balance and the stable movement [11–13]. Current hypothesis was that the complete link from a motor command to its concurrent muscular control was possibly assessed by a specific animal model and a proper behavioral test, and the adopted indicator and UL model revealed the link. Especially, the proposed model was evaluated by additional tests, such as RR and OSD, which were generally used to identify the functional abnormality in vestibular system. Thus, current study was expected to show how the damaged neural motor command affected the postural and the motional balance by assessing the indicators, and fulfill the incomplete series of the neuroanatomical connection from the damaged vestibular end organ to its concurrent muscular responses to maintain the postural and the motional balance.

### 4.1 Effects of vestibular imbalance on hindlimb

For a quadruped like a rat, a stable balance of posture or voluntary movement requires a well-harmonized coordination of muscular activities. Various skeletal muscles are located in the front and hindlimbs, and the core muscles are the medical

head of triceps branchii (TM), the long head of triceps branchii (TL), the vastus lateralis (VL), the vastus intermedius (VI), the gastrocnemius (GL), and the soleus [28]. Based on the vestibular neural responses to a kinetic perturbation as well as the muscular functions, the dominant role for the postural balance was believed to be conducted by the hindlimb [29]. Especially, due to its concurrent activity during a balance control, the soleus muscle and the medial GL in the hindlimb were often pointed as the mainly converging areas of motor commands to build up the balance for posture and voluntary movement [23, 24, 26, 30]. In some examinations for the relation between the skeletal muscles and a stable posture, the soleus H-reflex also indicated that the modulation shifted to the decrease in its amplitude while other fine motor commands were accumulated in the main command [29, 31, 32]. In addition, the functional differences in the muscles were revealed by the intrinsic physiological characteristics and the muscular geometry as well as the biased sensory feedback [24, 33, 34]. Unilateral labyrinthectomy (UL) or bilateral labyrinthectomy (BL) showed no evidence to affect the morphological changes in the skeletal muscles [23]. Nevertheless, the labyrinthectomy paralyzed the hindlimb by increasing the PW as shown in Fig. 3. Our fundamental finding in this study demonstrated the direct relation between the vestibular end organ and the postural balance supported by the skeletal muscles. According to the previous study [23], the abnormal balance and the reduced walking performance that we observed after UL were possibly caused by the neural failure in the motor commands, instead of the alterations in the muscular properties. In normal condition, the motor command to control the skeletal muscles in the hindlimb was mainly covered by the slow twitching muscle fibers, which the soleus contained up to 50% [28]. During the perturbation in posture, however, the portion by the soleus in the motor command was reduced, and it was replaced by additionally recruited neural information from different central nervous areas. The vestibular nuclei would be one of the critical central regions to provide the neural information based on the three-dimensional head movements. If the peripheral vestibular structure became malfunctioned, it implied some sources for the removed information in the motor command were absent. Considering that the vestibular stimulation mainly affected the responses in medial GL more than the soleus [24], the increased HPW was resulted by the partially missing information to the medial GL, initiated from the vestibular end organ. Thus, the abnormal posture in PW after UL was caused by the skeletal muscles with a large proportion of fast twitching fibers, like the medial GL (Fig. 4).

### 4.2 Mechanism behind the chemical labyrinthectomy

In medical treatments, chemical intratympanic injection is a common method for the treatment of vestibular related



**Fig. 4** Schematic overview from vestibular damage to dysfunctional motor control. The destruction of the vestibular hair cells by a chemical injection generated the mismatched neural information from both sides of ear. These unbalanced vestibular signals were transmitted through the vestibular nuclei (VN), and they were descended to the muscles

diseases. Although the effects on different vestibular inner organs depended on the type of chemicals, the approach was widely used to reduce the burdens by a surgical way [35, 36]. As only small amount of the injected toxic solution was expected to be absorbed to vestibular epithelia through the semi-permeable membrane of the round and the oval windows [37], the solution in the middle ear cavity should be remained for an enough duration (e.g., 20–30 min in our current experiment). Generally, the absorbing amount of the solution depended on the diffusing windows and the concentration of the solution [37–39]. The structural shape and the various perilymphatic flows in the labyrinth as well as the molecular weight were considered the critical factors to affect the absorbing amount of the chemical solution [37, 40, 41]. Including these mechanical properties, a general osmotic delivery through a semi-permeable material indicated the contacting area as well as the pressure caused by the solution also increased the absorbing amount of the solution. Thus, the amount of the solution filled in the middle ear cavity was decided to provide two factors, increasing the contacting area and the pressure by the solution. However, the injecting amount should be limited due to the eustachian tube connecting between the middle ear and the stomach. When the amount was overflowed, it easily flew into the stomach, causing a fatal consequence [42, 43]. Thus, a moderate amount of the toxic solution was determined based on the volume of the middle ear cavity, and it contributed a lower chance for an animal's death during the injection.

## 5 Conclusion

This study investigated the effects by the physical suppression of the peripheral vestibular system, focusing on the postural imbalance. Particularly, the dysfunctional responses in postural control after UL were examined based on PW, which directly represented the effects. The destruction of the hair cells

following the lateral vestibulospinal track. The serial neural connectivity from the labyrinth to the lower limb muscles described the circumstance of the abnormal PWs. According to previous studies, the major anatomical connectivity was identified in the soleus muscle, located in the lower limb

in the vestibular end organ caused the walking imbalance by the dysfunctional motor controls, and it resulted in the reduction of the sustaining time on the rolling rod. According to the results of RR and PW, the abnormal performance in walking on the rolling rod was possibly initiated by the unstable posture as shown in PW. Especially, the neural connectivity from the vestibular nuclei to the motors suggested that the vestibular damages affected PW in the hind more than that in the front paw. Our experimental results of PW indicated the changed posture, and it provided the neuroanatomical explanation to clarify the behavioral consequences of RR. The addressed connection was also expected to describe the postural imbalance by neurological disorders related with the vestibular system, and it could be a critical source to understand the underlying mechanism in the postural controls.

**Funding** This research was supported by Basic Science Research Program through the National Research Foundation of Korea (NRF) funded partially by the Ministry of Education (2018R1A6A1A03025523 & 2019R111A1A01041450).

## References

1. Claret CR, Herget GW, Kouba L, Wiest D, Adler J, Tschamer V, Stieglitz T, Pasluosta C (2019) Neuromuscular adaptations and sensorimotor integration following a unilateral transfemoral amputation. *J Neuroeng Rehabil* 16(1):115. <https://doi.org/10.1186/s12984-019-0586-9>
2. Kim G, Kim K-S, Lee S (2017) The integration of neural information by a passive kinetic stimulus and galvanic vestibular stimulation in the lateral vestibular nucleus. *Med Biol Eng Comput* 55(9): 1621–1633
3. Appiah-Kubi KO, Wright WG (2019) Vestibular training promotes adaptation of multisensory integration in postural control. *Gait Posture* 73:215–220
4. Paulus WM, Straube A, Brandt T (1984) Visual stabilization of posture. Physiological stimulus characteristics and clinical aspects. *Brain* 107(Pt. 4):1143–1163

5. Simoneau M, Teasdale N, Bourdin C, Fleury M, Nougier V (1999) Aging and postural control: postural perturbations caused by changing the visual anchor. *J Am Geriatr Soc* 47(2):235–240
6. Berela AMF, Caporicci S, de Freitas PB, Jeka JJ, Barela JA (2018) Light touch compensates peripheral somatosensory degradation in postural control of older adults. *Hum Mov Sci* 60:122–130
7. Lhomond O, Teasdale N, Simoneau M, Mouchnino L (2016) Neural consequences of increasing body weight: evidence from somatosensory evoked potential and the frequency-specificity of brain oscillations. *Front Hum Neurosci* 10:318. <https://doi.org/10.3389/fnhum.2016.00318>
8. Wallace JW, Rasman BG, Dalton BH (2018) Vestibular-evoked responses indicate a functional role for intrinsic foot muscles during standing balance. *Neurosci*. 377:150–160
9. Mergner T, Schweigart G, Fennell L, Maurer C (2009) Posture control in vestibular-loss patients. *Ann N Y Acad Sci* 1164:206–215
10. Waterston JA, Bames GR (1992) Visual-vestibular interaction during head-free pursuit of pseudorandom target motion in man. *J Vestib Res* 2(1):71–88
11. Horak FB (2009) Postural compensation for vestibular loss. *Ann N Y Acad Sci* 1164:76–81
12. Curthoys IS, Halmagyi GM (1995) Vestibular compensation: a review of the oculomotor, neural and clinical consequences of lateral vestibular loss. *J Vestib Res* 5(2):67–107
13. Manzari L, Burgess AM, MacDougall HG, Curthoys IS (2013) Vestibular function after vestibular neuritis. *Int J Audiol* 52(10):713–718
14. Peterka RJ, Statler KD, Wrisley DM, Horak FB (2011) Postural compensation for unilateral vestibular loss. *Front Neurol* 2:57. <https://doi.org/10.3389/fneur.2011.00057>
15. Hamm RJ, Pike BR, O'Dell DM, Lyeth BG, Jenkins LW (1994) The rotarod test: an evaluation of its effectiveness in assessing motor deficits following brain injury. *J Neurotrauma* 11(2):187–196
16. Jadhav RS, Ahmed L, Swamy PL, Sanaullah S (2013) Neuroprotective effects of polyhydroxy pregnane glycoside isolated from *Wattakaka volubilis* (L.f.) straph. After middle cerebral artery occlusion and reperfusion in rats. *Brain Res* 1515:78–87
17. Chaniary KD, Baron MS, Rice AC, Wetzel PA, Ramakrishnan V, Shapiro SM (2009) Quantification of gait in dystonic Gunn rats. *J Neurosci Methods* 180(2):273–277
18. Macpherson JM (1994) Changes in a postural strategy with inter-paw distance. *J Neurophysiol* 71(3):931–940
19. Honeycutt CF, Gottschall JS, Nicholas TR (2009) Electromyographic responses from the hindlimb muscles of the decerebrate cat to horizontal support surface perturbations. *J Neurophysiol* 101(6):2751–2761
20. Giszter SF, Davies MR, Graziani V (2007) Motor strategies used by rats spinalized at birth to maintain stance in response to imposed perturbations. *J Neurophysiol* 97(4):2663–2675
21. Alford EK, Roy RR, Hodgson JA, Edgerton VR (1987) Electromyography of rat soleus, medial gastrocnemius, and tibialis anterior during hind limb suspension. *Exp Neurol* 96(3):635–649
22. Tan U (1985) Relationships between head skill and the excitability of motoneurons innervating the postural soleus muscle in human subjects. *Int J Neurosci* 26(3–4):289–300
23. Kasri M, Picquet F, Falempin M (2004) Effects of unilateral and bilateral labyrinthectomy on rat postural muscle properties: the soleus. *Exp Neurol* 185(1):143–153
24. Dakin CJ, Héroux ME, Luu BL, Inglis JT, Blouin JS (2016) Vestibular contribution to balance control in the medial gastrocnemius and soleus. *J Neurophysiol* 115(3):1289–1297
25. Loram ID, Maganaris CN, Lakie M (2005) Human postural sway results from frequent, ballistic bias impulses by soleus and gastrocnemius. *J Physiol* 564(Pt.1):295–311
26. Héroux ME, Dakin CJ, Luu BL, Inglis JT, Blouin JS (2014) Absence of lateral gastrocnemius activity and differential motor unit behavior in soleus and medial gastrocnemius during standing balance. *J Appl Physiol* 116(2):140–148
27. Vieri TM, Loram ID, Muceli S, Merletti R, Farina D (2012) Recruitment of motor units in the medial gastrocnemius muscle during human quiet standing: is recruitment intermittent? What triggers recruitment? *J Neurophysiol* 107(2):666–676
28. Hawes ML, Kennedy W, O'Callaghan MW, Thurberg BL (2007) Differential muscular glycogen clearance after enzyme replacement therapy in a mouse model of Pompe disease. *Mol Genet Metab* 91(4):343–351
29. Murray AJ, Croce K, Belton T, Akay T, Jessell TM (2018) Balance control mediated by vestibular circuits directing limb extension or antagonist muscle co-activation. *Cell Rep* 22(5):1325–1338
30. Domen K, Kawaiishi Y (2016) The relationship between dynamic balancing ability and posture-related modulation of the soleus H-reflex. *J Electromyogr Kinesiol* 26:120–124
31. Angulo-Kinzler RM, Mynark RG, Koceja DM (1998) Soleus H-reflex gain in elderly and young adults: modulation due to body position. *J Gerontol A Biol Sci Med Sci* 53(2):M120–M125
32. Earles DR, Koceja DM, Shively CW (2000) Environmental changes in soleus H-reflex excitability in young and elderly subjects. *Int J Neurosci* 105(1–4):1–13
33. Fukunaga T, Roy RR, Shellock FG, Hodgson JA, Day MK, Lee PL, Kwong-Fu H, Edgerton VR (1992) Physiological cross-sectional area of human leg muscles based on magnetic resonance imaging. *J Orthop Res* 10(6):928–934
34. Hoy MG, Zajac FE, Gordon ME (1990) A musculoskeletal model of the human lower extremity: the effect of muscle, tendon, and moment arm on the moment-angle relationship of musculotendon actuators at the hip, knee, and ankle. *J Biomech* 23(2):157–169
35. Guthrie ONW (2008) Aminoglycoside induced ototoxicity. *Toxicol*. 249(2):91–96
36. Yazdandshenas H, Ashouri A, Kaufman G (2016) Neurovestibular compensation following ototoxic lesion and labyrinthectomy. *Intern Arch Otorhinolaryngol* 20(2):114–123
37. Takumida M, Anniko M (2004) Localization of endotoxin in the inner ear following inoculation into the middle ear. *Acta Otolaryngol* 124(7):772–777
38. Schoo DP, Tan GX, Ehrenburg MR, Pross SE, Ward BK, Carey JP (2017) Intratympanic (IT) therapies for Menière's disease: some consensus among the confusion. *Curr Otorhinolaryngol Rep* 5(2):132–141
39. Vignaux G, Chabbert C, Gaboyard-Niay S, Travo C, Machado ML, Denise P, Comoz F, Hitier M, Landemore G, Philoxène B, Besnard S (2012) Evaluation of the chemical model of vestibular lesions induced by arsanilate in rats. *Toxicol Appl Pharmacol* 258(1):61–71
40. Zhang Y, Zhang R, Dai C, Steyger PS, Yu Y (2010) Comparison of gentamicin distribution in the inner ear following administration via the endolymphatic sac or round window. *Laryngoscope* 120(10):2054–2060
41. Plontke SK, Mynatt R, Gill RM, Borgmann S, Salt AN (2007) Concentration gradient along the scala tympani after local application of gentamicin to the round window membrane. *Laryngoscope* 117(7):1191–1198
42. Wu ML, Tsai WJ, Ger J, Deng JF (2003) Clinical experience of acute ferric chloride poisoning. *Vet Hum Toxicol* 45(5):243–246
43. Menendez JM, Abramson L, Vera R, Duza G, Palermo M (2015) Total gastrectomy due to ferric chloride intoxication. *Acta Gastroenterol Latinoam* 45(3):212–216

**Publisher's note** Springer Nature remains neutral with regard to jurisdictional claims in published maps and institutional affiliations.





**Gyutae Kim** received a Ph.D. in Electrical Engineering from Old Dominion University, US in 2011. In the same year, he started to work as a postdoctoral researcher focusing on the motor control in the cerebellar cortex at Washington University, St Louis, US. In 2014, he joined as a research professor at the institute of information and Electronic research in Inha University, Korea. His current work focuses on the transmission and integration of neural information in the vestibular system.



**Kyu-Sung Kim** received a bachelor and master degrees for medical doctor in 1991 and 1996, and received a Ph.D. in Otolary, 2006. Since 2003, he has worked as professor and medical doctor at the Department of Otolaryngology, Inha University Hospital. In 2005–2007, he joined as a visiting scholar in other universities (Tokushima University, Japan & the Johns Hopkins University, US), and academically cooperated with the research staffs. Now, he is the chairman in the Department of

Otolaryngology, and also the director of the Institute of Aerospace Medicine at Inha University hospital.



**Nguyen Nguyen** received a bachelor and resident doctor degrees for medical doctor in 2011 and 2014, and received a Ph.D. in Otolaryngology at Inha University in 2020. Since 2014, he has worked as a professor and medical doctor at the Department of Otolaryngology, Hue University of Medicine and Pharmacy, Vietnam. In 2016-2017, he joined as a medical doctor in Fellowship program at Inha university, Korea. He is currently working as the Departmental Deputy Head of Otolaryngology, Hue University

of Medicine and Pharmacy, Vietnam.